4-1-1998

The CArG Boxes in the Promoter of the Arabidopsis Floral Organ Identity Gene APETALA3 Mediate Diverse Regulatory Effects

Joline J. Tilly
Dartmouth College

David W. Allen
Dartmouth College

Thomas Jack
Dartmouth College

Development 125, 1647-1657 (1998)
Printed in Great Britain © The Company of Biologists Limited 1998
DEV0159

The CArG boxes in the promoter of the *Arabidopsis* floral organ identity gene *APETALA3* mediate diverse regulatory effects

Joline J. Tilly, David W. Allen and Thomas Jack*

Department of Biological Sciences, Dartmouth College, Hanover, NH 03755, USA
*Author for correspondence (e-mail: thomas.jack@dartmouth.edu)

Accepted 26 February; published on WWW 1 April 1998

SUMMARY

APETALA3 **is a MADS box gene required for normal development of the petals and stamens in the *Arabidopsis* flower. Studies in yeast, mammals and plants demonstrate that MADS domain transcription factors bind with high affinity to a consensus sequence called the CArG box. The *APETALA3* promoter contains three close matches to the consensus CArG box sequence. To gain insights into the *APETALA3* regulatory circuitry, we have analyzed the *APETALA3* promoter using *AP3*::*uidA*(GUS) fusions. 496 base pairs of *APETALA3* promoter sequence 5′ to the transcriptional start directs GUS activity in the same temporal and spatial expression pattern as the *APETALA3* RNA and protein in wild-type flowers. A synthetic promoter consisting of three tandem repeats of a 143 base pair sequence directs reporter gene activity exclusively to petals and stamens in the flower. We have analyzed the role of the CArG boxes by site-specific mutagenesis and find that the three CArG boxes mediate discrete regulatory effects. Mutations in CArG1 result in a decrease in reporter expression suggesting that CArG1 is the binding site for a positively acting factor or factors. Mutations in CArG2 result in a decrease in reporter expression in petals, but the expression pattern in stamens is unchanged. By contrast, mutations in CArG3 result in an increase in the level of reporter gene activity during early floral stages suggesting that CArG3 is the binding site for a negatively acting factor.**

Key words: *Arabidopsis*, Flower development, *APETALA3*, CArG box

INTRODUCTION

The developmental fate of the organs in the *Arabidopsis* flower is controlled by the homeotic floral organ identity genes. When the activity of a particular floral organ identity gene is lost due to mutation, there is a homeotic conversion of one organ type to another. For example, the *APETALA3* (*AP3*) and *PISTILLATA* (*PI*) genes are necessary for the proper development of petals that develop in the second whorl and stamens that develop in the third whorl of the flower. In *ap3* and *pi* mutants, sepals and carpels develop in positions normally occupied by petals and stamens respectively (Bowman et al., 1989; Jack et al., 1992). Accumulating genetic and molecular evidence suggests that the AP3 and PI proteins together make up the B class organ identity function and these two proteins are sufficient to direct the identity of petals and stamens in the flower. In support of this, ectopic expression of *AP3* and/or *PI* throughout the flower leads to homeotic transformations. Specifically misexpression of *AP3* (i.e. 35S::AP3) results in the development of stamens in place of carpels in the fourth whorl and misexpression of *PI* (i.e. 35S::PI) results in the development of petaloid sepals in place of sepals in the first whorl of the flower (Jack et al., 1994; Krizek and Meyerowitz, 1996). 35S::AP3 leads to fourth whorl organ identity changes because *PI* is transiently expressed in whorl four during early stages of flower development (Goto and Meyerowitz, 1994). Similarly, 35S::PI leads to partial transformations of the first whorl because *AP3* is expressed in a small number of cells on the adaxial surface at the base of the first whorl sepals (Weigel and Meyerowitz, 1993). When both *AP3* and *PI* are ectopically expressed together (35S::AP3 35S::PI), the homeotic transformations are complete; 35S::AP3 35S::PI flowers consists of two outer whorls of petals and two inner whorls of stamens (Krizek and Meyerowitz, 1996).

Both AP3 and PI proteins contain a conserved protein coding domain called the MADS domain (Jack et al., 1992; Goto and Meyerowitz, 1994). The MADS domain is found in a number of well-characterized transcription factors, such as MCM1 in yeast (Passmore et al., 1988) and SERUM RESPONSE FACTOR (SRF) and MEF2A in mammals (Treisman, 1986; Shore, 1995). The MADS box is also present in a number of developmental control genes in a variety of plant species (Schwarz-Sommer et al., 1990; Weigel and Meyerowitz, 1994; Yanofsky, 1995; Purugganan et al., 1995; Theißen et al., 1996). At present, more than 20 MADS box genes have been isolated in *Arabidopsis*; six of which have been correlated with a mutant phenotype: *AP3* (Jack et al., 1992), *PI* (Goto and Meyerowitz, 1994), *AGAMOUS* (*AG*; Yanofsky et al., 1990), *APETALA1* (*AP1*; Gustafson-Brown et al., 1994), *CAULIFLOWER* (*CAL*; Kempin et al., 1995), and *AGL5* (Kempin et al., 1997). The function of the remaining

MADS box genes is less well understood since loss-of-function mutants are not presently available (Ma et al., 1991; Rounsley et al., 1995).

All of the MADS domain proteins tested to date are sequence-specific DNA binding proteins which bind to DNA as dimers (reviewed by Riechmann and Meyerowitz, 1997). In all proteins tested, the MADS domain has been found to be necessary for DNA binding in vitro (Shore, 1995) and to be important, though not absolutely essential, for dimerization (Pellegrini et al., 1995; Davies et al., 1996). MADS domain proteins bind to a family of closely related ten base pair sequences that are referred to as the CArG box ($CC(A/T)_6GG$; Dolan, 1991; Treisman, 1992). Many of the plant MADS domain proteins bind in vitro to the CArG box sequence as either homodimers or heterodimers (Schwarz-Sommer et al., 1992; Tröbner et al., 1992; Huang et al., 1993; Shiraishi et al., 1993; Savidge et al., 1995; Zachgo et al., 1995; Mizukami et al., 1996; Riechmann et al., 1996a,b; Davies et al., 1996; Huang et al., 1996). Sequencing of the *AP3* promoter reveals three sequences between −90 and −180 with a nine out of ten match with the CArG box consensus sequence (Okamoto et al., 1994).

In particular, we are interested in understanding how expression of the floral organ identity gene *AP3* is controlled. *AP3* RNA initially appears in very young flowers in the precursor cells for the petals and stamens, (at floral stage 3 of Smyth et al., 1990) and once activated *AP3* RNA continues to be expressed in the petals and stamens throughout most of flower development (Jack et al., 1992). Initial establishment of *AP3* expression is thought to be due to transiently expressed factors such as the meristem identity genes *LEAFY (LFY)* and *UNUSUAL FLORAL ORGANS (UFO)* (Weigel et al., 1992; Ingram et al., 1995; Lee et al., 1997). In both *lfy* and *ufo* mutants, the domain and the level of expression of *AP3* and *PI* are reduced, reflecting the formal role of *LFY* and *UFO* as positive regulators of *AP3* and *PI* (Weigel and Meyerowitz, 1993; Levin and Meyerowitz, 1995). After *AP3* and *PI* are activated, expression in petals and stamens is maintained by an autoregulatory circuit that is dependent on both *AP3* and *PI* (Schwarz-Sommer et al., 1992; Jack et al., 1994; Zachgo et al., 1995; Krizek and Meyerowitz, 1996).

To examine in more detail how *AP3* is controlled, we have undertaken a detailed analysis of the *AP3* promoter using fusions to the *uidA* reporter gene. The *AP3* promoter contains discrete elements which we demonstrate are necessary, and when placed upstream of a minimal promoter, are sufficient for distinct aspects of the *AP3* pattern. We also constructed a synthetic *AP3* promoter that consists of a tandem repeat of a 143 base pair segment of the *AP3* promoter that contains the three CArG boxes. We demonstrate that the CArG box sequences in the *AP3* promoter are not functionally equivalent and that the CArG boxes mediate both positive and negative effects on both the establishment and maintenance circuits of the *AP3* expression pattern.

MATERIALS AND METHODS

Construction of pD991 and pD343

Two key plant transformation plasmids are pD991 (minimal promoter::GUS-3′NOS) and pD343 (promoterless GUS-3′NOS). The minimal promoter that we used to construct pD991 was the −60 promoter from the 35S gene of cauliflower mosaic virus. This minimal promoter contains a TATA box but by itself is not capable of directing detectable levels of transcription. The −60CaMV::GUS-3′NOS region is derived from pBIN421.9 (Clontech). To create plasmid pD991, a 2.2 kb fragment from pBIN421.9 was cloned into the binary plant transformation vector pCGN1547 (McBride and Summerfelt, 1990). The promoterless GUS-3′NOS transformation plasmid pD343 was made by cloning a 2.2 kb fragment from pBI101.2 (Clontech) into pCGN1547. Details of the plasmid constructions are available on request.

5′ deletions of the *AP3* promoter

We constructed both transcriptional and translational fusions of *AP3* to *uidA*. Transcriptional fusions contain *AP3* promoter sequences 5′ to the transcription start site but do not contain the 5′UTR of AP3. For the transcriptional fusions, PCR of an *AP3* genomic clone was used to isolate *AP3* promoter fragments beginning at −1 (Jack et al., 1992). The translational fusions are fused at the ATG for GUS and thus contain the 5′ UTR of *AP3* (Jack et al., 1994). We have not observed any differences in the GUS activity patterns when comparing transcriptional and translational fusions. The best evidence in support of this is the comparison of fusions that contain –332 or –650 of the *AP3* promoter; in both cases the transcriptional and translational constructs gave an identical temporal and spatial GUS activity pattern. Details of plasmid constructions are available on request.

Fusions of *AP3* promoter fragments fused to –60CaMV::GUS

AP3 promoter fragments were cloned in both orientations 5′ to a –60CaMV::GUS in pD991. To make the −83 to −225 trimers, the –83 to –225 *Ava*II fragment was isolated, filled-in with Klenow, and cloned into the pGEM7z(+)/SmaI. The orientation of the fragment in pGEM was then determined using PCR. Trimers of the –83 to –225 fragment were made by digesting these plasmids with various combinations of restriction enzymes and performing four-way ligations. The nature of these ligations enabled us to direct the precise orientation of the fragments relative to each other and relative to the pGEM vector; this ensured that the promoter pieces would all be oriented in the same direction. These trimers were then cut out of the pGEM plasmid and cloned into pD991. Trimers of the –225 to –330 and –330 to –496 promoter regions were similarly constructed.

Site-specific mutagenesis of CArG boxes in the *AP3* promoter

Site-directed mutagenesis was performed using the technique of Deng and Nickoloff (1992). Nucleotides were changed based on the conservation of the CC and GG dinucleotides in CArG boxes characterized in studies using SRF, MCM1, AG and AGL1-3 (Fig. 4A; Leung and Miyamoto, 1989; Pollock and Treisman, 1990; Wynne and Treisman, 1992; Shiraishi et al., 1993; Huang et al., 1993, 1995, 1996). The mutagenic primers that we used were as follows:

CArG1 (oligo AP3-77) 5′ TAAGTGATAAATTTT**AA**ATTTA-**TGT**AAACTG 3′

CArG2 (oligo AP3-80) 5′ AGTATTGCCTAAT**TA**ATGAAAG-**G**TAAGT 3′

CArG3 (oligo AP3-75) 5′ GAGTTA**CTAAAAATTT**AAAGTAT-TGCC 3′.

Mutagenized base pairs are underlined and the CArG consensus is in bold. For mutagenesis, the template plasmid was pD502 (a pGEM7z+ derivative which contained −1 to −496 of the *AP3* promoter). To verify that the mutations were present, the clones were sequenced on an ABI 373A automated DNA sequencer.

Agrobacterium-mediated transformation

AP3::GUS fusions in binary transformation vectors were transformed

into *Agrobacterium* strain ASE using the freeze-thaw method. To ensure that the *Agrobacterium* strain contained the correct AP3::GUS fusion, *Agrobacterium* DNA was isolated and the presence of the construct was determined by PCR using oligonucleotides specific for GUS and a region of the pCGN1547 transformation vector adjacent to the right border. Transgenic plants were generated by either root transformation (Valvekens et al., 1988) or vacuum infiltration (Bechtold et al., 1993) following standard protocols. For each construct (unless otherwise noted), at least ten independent lines were generated and analyzed. Copy number of representative lines was analyzed via genomic Southern using an *uidA* probe. The majority of representative lines contained a single T-DNA insertion and in only one case did we identify a line with more than four insertions. In individual representative lines that contained the same construct, but had different numbers of T-DNA insertions, we observed no difference in the GUS staining pattern.

GUS staining, microscopy and image processing

Inflorescences were stained and sectioned according to the protocol described by Sieburth et al. (1997). Images were acquired using an Optronix DEI-750 video camera connected to a Zeiss Axioskop microscope. Images were processed and assembled using Adobe Photoshop software.

Electrophoretic mobility shift assays

53 bp double stranded fragments containing CArG1 (5′-GTAATTAAA-AAAATCAGTTTACATAAATGGAAAATTTATCACTTAGTTTT-3′), CArG2 (5′-TTTCATCAACTTCTGAACTTACCTTTCATGGATTA-GGCAATACTTTCCA-3′), and CArG3 (5′-TGGATTAGGCAA-TACTTTCCATTTTTAGTAACTCAAGTGGACCCTTTAC-3′) were isolated by PCR amplification and cloned into pGEM7z(+)/SmaI. DNA fragments were end labeled using T4 polynucleotide kinase (NEB) and [γ-^{32}P]ATP. AP3 and PI proteins were produced by in vitro transcription/translation using TNT® Coupled Reticulocyte Lysate System (Promega) using template plasmids pSPUTK-AP3 and pSPUTK-PI (gifts from Jose Luis Riechmann). EMSA assays were performed according to Riechmann et al. (1996a,b).

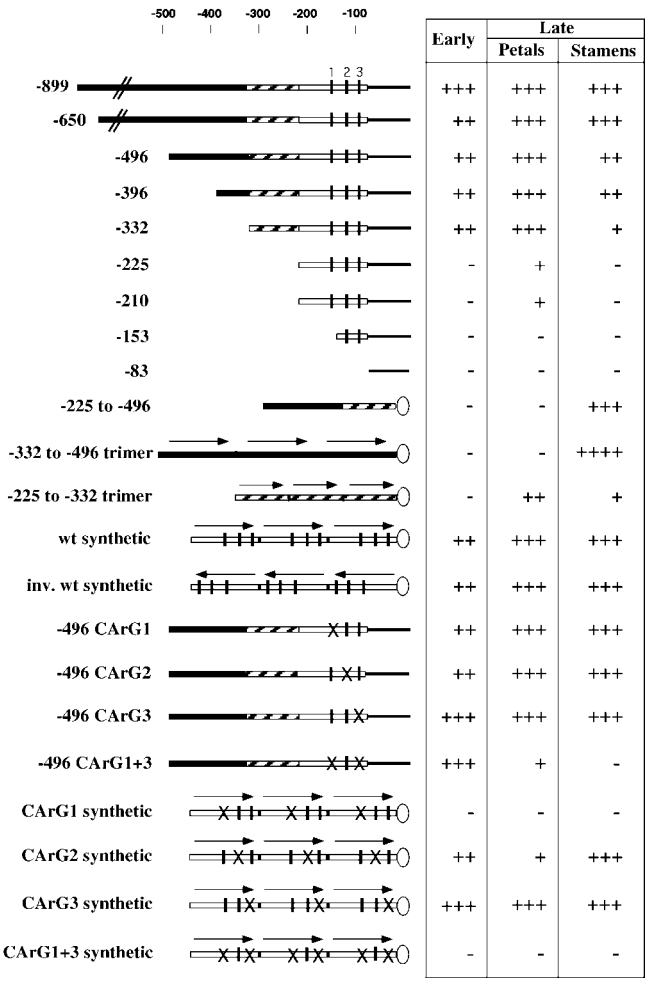

Fig. 1. Summary of constructs analyzed. Schematic diagrams of the AP3::GUS constructs analyzed, and the spatial (petal and stamen) and temporal expression pattern observed. Early stages are defined as stages 3-5, late as stages 6-10. The oval indicates fusions to the –60 CaMV minimal promoter. Vertical bars indicate the position of three CArG box sequences. X indicates CArG box mutations. Arrows indicate orientation of multimerized fragments.

RESULTS

5′ deletions in the *AP3* promoter reveal the presence of organ-specific elements

We are primarily interested in understanding how *AP3* expression is established and maintained in the flower. If we assume that these effects are transcriptional, then the positive and negative regulatory inputs are most likely mediated through the *AP3* promoter. The basic technique we used to identify *cis*-acting regulatory regions in the promoter is fusion of the *AP3* promoter to the *uidA* reporter gene which encodes the bacterial enzyme β-glucuronidase or GUS (Jefferson et al., 1987). The *AP3* promoter::GUS fusion constructs (AP3::GUS) were stably transformed into *Arabidopsis* by either root transformation (Valvekens et al., 1988) or vacuum infiltration (Bechtold et al., 1993). For all constructs (unless otherwise noted) we analyzed at least ten independent transgenic lines. For many constructs we observed variability in the pattern of GUS activity when comparing independent lines derived from the same construct. The results presented here represent the typical pattern observed (i.e. found in at least 70% of the lines examined unless otherwise indicated). A summary of the constructs analyzed is shown in Fig. 1.

To determine the location of the major controlling elements in the *AP3* promoter, we made a series of 5′ deletions in the promoter (Fig. 1). Previous experiments demonstrated that 3.7 kilobases (kb) 5′ to the *AP3* translation start site along with 1.5 kb of sequences 3′ to the *AP3* polyA sites were sufficient to give a GUS expression pattern that was indistinguishable from the *AP3* RNA and protein expression pattern in wild-type flowers during floral stages 7-8 (Jack et al., 1994). Additional information about the *AP3* promoter comes from mutant rescue experiments: in one case 1.7 kb of the *AP3* promoter fused to an *AP3* cDNA rescues strong *ap3* mutants (Irish and Yamamoto, 1995) and in a second case a genomic fragment containing approximately 850 base pairs of 5′ promoter sequences plus 3 kb of 3′ sequences rescues the weak *ap3-1* mutant (Okamoto et al., 1994).

5′ deletions in the *AP3* promoter to –899, –650, or –496 result in GUS activity in a spatial and temporal pattern identical to the construct that contains 3.7 kb of 5′ and 1.5 kb of 3′ sequences demonstrating that 3′ *AP3* sequences do not direct spatial and temporal patterning information (Figs 1, 2A,B).

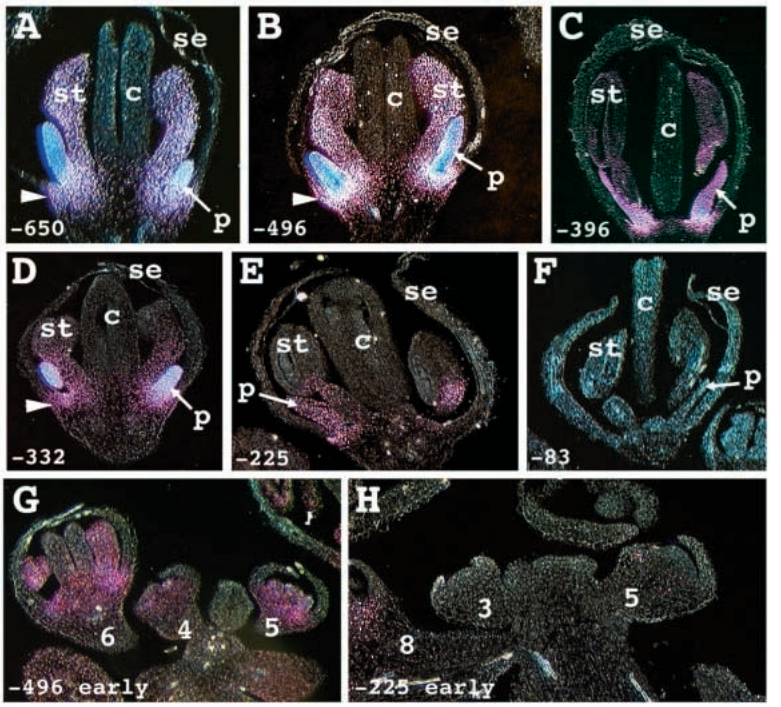

Fig. 2. 5′ Deletions in the *AP3* promoter. (A) Single stage 8 flower with an AP3::GUS fusion containing 650 bases of 5′ sequences, which directs a high level of GUS activity to petals and stamens. Arrowhead points to GUS activity at the base of the first whorl organs. (B) Single stage 8 flower with an AP3::GUS fusion containing 496 bases of 5′ sequences, which directs a high level of GUS activity to petals and stamens. Arrowhead points to GUS activity at the base of the first whorl organs. (C) Single stage 9 flower with an AP3::GUS fusion containing 396 bases of 5′ sequences, which directs a high level of GUS activity to petals. The level of GUS activity in stamens is comparatively lower. (D) Single stage 8 flower with an AP3::GUS fusion containing 332 bases of 5′ sequences, which directs a high level of GUS activity to petals. A very low level of GUS activity is detectable in stamens. Arrowhead points to GUS activity at the base of the first whorl organs. (E) Single stage 8 flower with an AP3::GUS fusion containing 225 bases of 5′ sequences, which directs a low level of GUS activity to petals and a very low level to a few cells in stamens beginning at stage 6. (F) Single stage 10 flower with an AP3::GUS fusion containing 83 bases of 5′ sequences, which fails to direct detectable GUS activity in the inflorescence. (G) Section through an inflorescence with 496 bases of 5′ *AP3* promoter sequences. GUS activity is detected beginning at floral stage 3. Here, stage 4, 5 and 6 flowers exhibit GUS activity in petal and stamen primordia. (H) Section through an inflorescence with 225 bases of 5′ *AP3* promoter sequences. GUS activity is not detected in the stage 3 and 5 flowers in this section. The stage 8 flower to the left exhibits a low level of GUS activity. Numbers indicate floral stage. se, sepal; p, petal; st, stamen; c, carpel.

Although the spatial and temporal pattern is the same when comparing −650 or −496 with −3.7, the level of expression during early stages is reduced with constructs that contain less than −727 of the *AP3* promoter (see accompanying paper by Hill et al., 1998). We analyzed the GUS activity patterns at earlier stages of flower development in transcriptional fusions containing −650 and −496 of the *AP3* promoter. To visualize the GUS activity patterns at earlier stages of flower development, we sectioned GUS-stained inflorescences and examined sections utilizing dark-field microscopy. GUS activity is detected beginning at stage 3 in the precursor cells of the petals and stamens in both −650 AP3::GUS and −496 AP3::GUS plants (Fig. 2G). During stages 3-6, GUS activity is expressed at an equivalent level in petal and stamen primordia. Beginning in stage 7, the level of GUS signal is lower in stamens compared to petals. At this stage, GUS activity is also clearly detectable in a small number of cells on the adaxial side at the base of the first whorl organs (arrowheads Fig. 2A,B). By stage 9, GUS activity is detectable at a very low level in stamens, and the level in petals is lower than that observed at earlier developmental stages. In stage 11, the level of GUS activity increases in stamen filaments, and by the beginning of stage 12, a high level of GUS activity is detected in both the filaments and anthers but it is no longer detectable in the petals. The −496 and −650 AP3::GUS fusions also direct GUS activity to ovules; more detailed information about the ovule patterns in various AP3::GUS constructs is described in the accompanying paper by Hill et al. (1998).

Constructs that contain −396 of the *AP3* promoter produce a spatial and temporal pattern of GUS activity that is indistinguishable from the −496 and −650 constructs, but the level of GUS activity in the stamens from the −396 construct is reduced compared to constructs that contain 496 base pairs (or more) of the promoter (Fig. 2C). 5′ deletions to −332 produce a more dramatic reduction in intensity of stamen staining compared to the −396 and −496 constructs (Fig. 2D), but early expression is unchanged. A further deletion to −225 dramatically reduces the staining intensity and alters the spatial and temporal expression pattern (Fig. 2E). Thirty percent of the −225 lines exhibit no staining, and the remaining lines exhibit very weak staining in petals and in a subset of cells of the stamens beginning at stage 6; early GUS activity is not detected in 5′ deletions to −225 (Fig. 2H). Further deletion to −210 results in an even higher percentage of non-staining lines (4 out of 6 lines generated exhibited no detectable staining, data not shown). The −210 lines that do show staining have a GUS pattern identical to those lines with 5′ deletions to −225. Further 5′ deletions to −153, −121, or −83 do not produce detectable GUS activity in the inflorescence (Fig. 2F).

Fusions of *AP3* promoter fragments fused to a minimal promoter

A second method used to assay for important regulatory regions in the *AP3* promoter is fusion of promoter pieces upstream of a minimal promoter fused to GUS. The minimal promoter we used is the first 60 base pairs of the 35S promoter of cauliflower mosaic virus (−60 CaMV) (Benfey and Chua, 1990). We constructed a large number of constructs that contained single promoter fragments fused to −60 CaMV::GUS and the majority of these constructs do not direct GUS activity to the flower (data not shown). The only promoter fragments that consistently direct GUS activity are ones that contained the promoter regions between −332 and −496. Some of these constructs contain promoter sequences both 5′ and 3′ to this

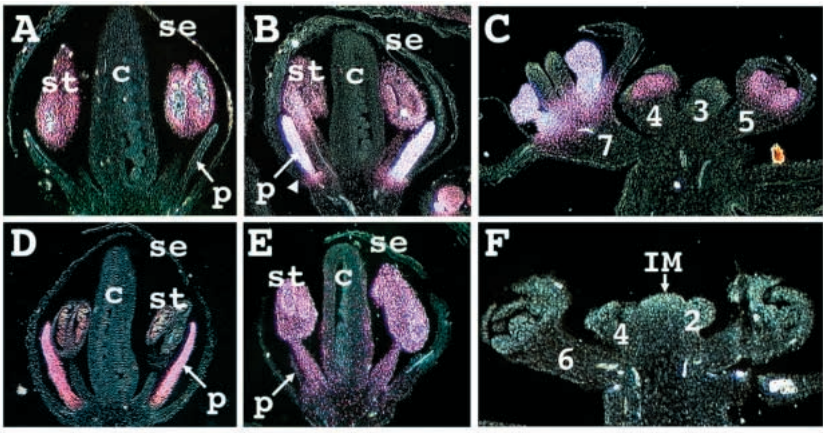

Fig. 3. A synthetic trimer of promoter sequences from –83 to –225 directs expression to petals and stamens. (A) Single stage 8 flower from a plant that contains an *AP3* promoter fragment from –225 to –496 cloned upstream of the minimal CaMV 35S –60 promoter::GUS; this construct directs GUS activity primarily to the anthers during mid to late stages of flower development. (B) Single stage 8 flower from a plant that contains a tandem trimer of *AP3* promoter sequences from –83 to –225, fused to –60 CaMV::GUS (synthetic AP3::GUS) directs a high level of GUS activity to petals and stamens. Note that GUS activity is not detected at the base of the first whorl organs (arrowhead). (C) Synthetic AP3::GUS (-83 to –225 trimer) inflorescence. GUS activity is first detectable in stage 4 flowers. (D) Single stage 10 flower from a plant that contains a tandem trimer of *AP3* promoter sequences from –225 to –332 fused to –60 CaMV::GUS. GUS activity is detected in petals and at a low level in stamens beginning at stage 6. (E) Single stage 9 flower from a plant that contains a tandem trimer of *AP3* promoter sequences from –332 to –496 fused to –60 CaMV::GUS. GUS activity is detected at a high level in stamens beginning at stage 7. (F) A –332 to –496 trimer –60 CaMV::GUS inflorescence. GUS activity is not detectable in flowers at stage 2, 4 or 6.

central core but every construct that contains the –332 to –496 sequence results in strong staining in anthers and comparatively weaker staining in stamen filaments from stages 9-12. A representative flower derived from a construct that contains sequences between –225 and –496 fused to –60 CaMV::GUS is shown in Fig. 3A.

A 143 base pair trimer that contains three CArG boxes recreates key aspects of the *AP3* pattern

Both 5′ deletions and fusions to a minimal promoter failed to implicate the three CArG box sequences in the *AP3* promoter between –90 and –180 as being either necessary or sufficient to direct high level expression of the reporter gene. Specifically, a 5′ deletion to –225 or to –210, which contains all three CArG box sequences, results in only very weak expression of GUS in the petals and stamens. A deletion to –153, which contains two of the CArG boxes (CArG2 and CArG3) fails to direct a detectable level of GUS activity. When a single copy of the –83 to –225 promoter piece that contains all three CArG box sequences is placed upstream of –60 CaMV::GUS, no GUS activity is detected in the inflorescences of transgenic plants (data not shown). To see if multiple copies of the CArG box containing fragment placed in tandem could direct expression of the reporter, we constructed dimers and trimers of the CArG box promoter region. Dimerization of the CArG box promoter region also failed to result in GUS activity in the flower (data not shown). However, when the –83 to –225 promoter piece is trimerized in tandem, a dramatic GUS activity pattern results (Fig. 3B,C). These synthetic AP3::GUS trimer constructs, in either wild-type or inverse orientations, direct GUS activity in a pattern that is very similar to the intact AP3::GUS fusions that contain 496 bases or more of the *AP3* promoter. Beginning at stages 3-4, synthetic AP3::GUS directs approximately equivalent levels of GUS activity in petal and stamen primordia and throughout developing petals and stamens through stage 8. The biggest difference between –496 AP3::GUS and synthetic AP3::GUS is the lack of detectable GUS activity in the adaxial cells at the base of the first whorl organs in synthetic AP3::GUS (Fig. 3B, compare with Fig. 2A, B). Beginning in stage 9, the level of GUS activity in anthers is comparatively lower than in petals. By stage 10, GUS activity is absent from the stamen (both anther and filament) and the level in the petals is lower compared to the level observed at earlier stages. By stage 11, GUS activity in the petals is no longer detectable. Also during stage 11, GUS activity is once again observed throughout the stamens, first in the stamen filaments and at a slightly later stage in the connective of the anthers. During stages 12-14, GUS activity is detectable in the connective of the stamen.

We also constructed and analyzed two other synthetic trimers (Fig. 1). One contained sequences between –225 and –332 and the second contained sequences between –332 and –496. A single copy of the –225 to –332 fragment cloned 5′ to –60 CaMV failed to direct detectable GUS activity in the flower. The –225 to –332 trimer produced GUS activity primarily in petals during mid-late stages of development (stages 6-9) but did not result in GUS activity at early stages (i.e. stages 3-5; Fig. 3D). A very low level of GUS activity was also occasionally observed in a subset of cells in the stamen between stages 6-9. The –332 to –496 trimer exhibited a spatial pattern identical to –332 to –496 monomers, but the level of GUS activity was comparatively higher in the trimer. Specifically, in the –332 to –496 trimer constructs, GUS activity was detected at a high level in anthers and at a low level in stamen filaments beginning at stage 9 (Fig. 3E,F).

Site-specific mutagenesis of the CArG boxes in the *AP3* promoter

Between –90 and –180 in the *AP3* promoter there are three sequences with similarity to the CArG box consensus sequence. These CArG box sequences are referred to as CArG1 (centered at –175), CArG2 (centered at –155) and CArG3 (centered at –98). The fact that a trimer containing the –83 to –225 promoter piece which contains all three CArG box sequences can direct expression of GUS in a spatial and temporal pattern similar to that directed by the intact *AP3* promoter suggested to us that the CArG box sequences could be mediating establishment and/or maintenance of the *AP3*

expression pattern. To assay the in vivo function of these CArG box sequences, we mutated the CArG box sequences in an attempt to reduce the ability of MADS domain transcription factors to bind. Oligonucleotide binding site selection experiments have been performed with the MADS domain proteins AG (Huang et al., 1993; Shiraishi et al., 1993), AGL3 (Huang et al., 1995), AGL1, and AGL2 (Huang et al., 1996). Using the AG protein, more than one hundred binding sites were selected and all the sequenced binding sites were similar to the CArG consensus sequence ($CC(A/T)_6GG$); in no case was an oligonucleotide selected that contained a mutation in the CC or GG dinucleotides at the ends of the ten base pair CArG consensus. Based on this evidence, we introduced two base pair mutations in all three CArG boxes, specifically targeting either the CC or GG dinucleotides (Fig. 4A). To test that we had diminished the ability of MADS domain proteins to bind to these mutant CArG boxes, we tested the ability of the AP3/PI heterodimer to bind to wild-type and mutant CArG box-containing DNA fragments in a electrophoretic mobility shift assay (EMSA). AP3 and PI proteins together, but neither protein alone, are able to bind to wild-type CArG1 and wild-type CArG3 (Fig. 4B). By contrast, DNA fragments that contain CArG1 or CArG3 mutations are not shifted when mixed with AP3 and PI proteins. In addition, we failed to detect binding of AP3 plus PI to either wild-type or mutant CArG2 containing DNA fragments.

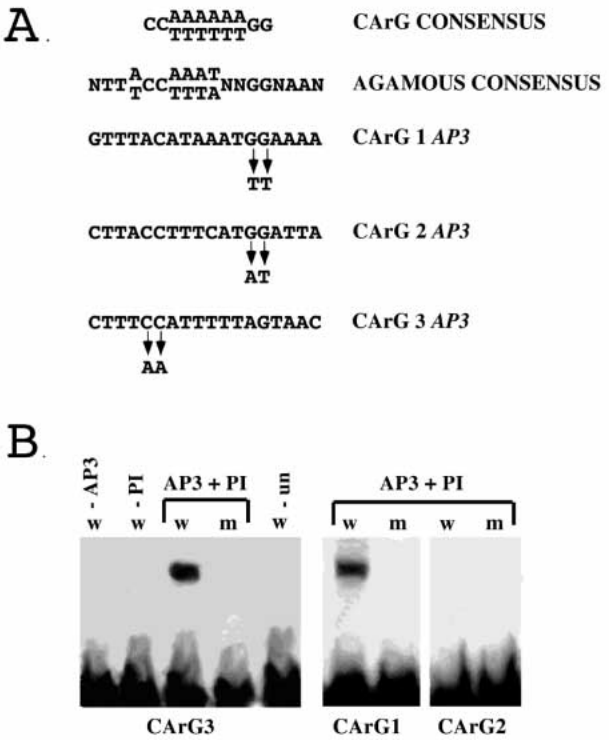

Fig. 4. In vitro DNA binding of AP3 and PI proteins to wild-type and mutant CArG boxes. (A) The top half of the figure is a schematic detailing the site-specific mutations that were constructed in the three CArG boxes in the *AP3* promoter. The top line shows the CArG consensus sequence, the second line the consensus binding sequence for the *Arabidopsis* MADS domain protein AG as determined by oligonucleotide selection experiments (Huang et al., 1993; Shiraishi et al., 1993), and the bottom three lines indicate the mutations that were constructed in CArG1, CArG2, and CArG3. (B) EMSA demonstrating that AP3 and PI together (AP3 + PI), but not AP3 or PI alone, bind to wild-type versions (w) of CArG1 (C1) and CArG3 (C3) but not to mutant versions (m) of CArG1 and CArG3. We did not detect binding of AP3 and PI to either wild-type or mutant CArG2 (C2). Unprogrammed (un) indicates result with transcription/translation lysate in the absence of plasmid.

To assay CArG box function in vivo, we fused *AP3* promoter pieces containing CArG box mutations to *uidA* and examined the GUS activity pattern in transgenic plants. We analyzed the effects of the CArG box mutations both singly and in combination in two different contexts: (1) in the context of the intact −496 promoter, and (2) in the context of the synthetic −83 to −225 trimer (in both wild-type and inverse orientations). The effects that we observed on the GUS activity pattern are described below.

CArG1 mutants

Mutations in CArG1 have a dramatic effect on the GUS pattern in the context of the synthetic promoter trimer but no observable effect in the context of the intact −496 promoter. CArG1 mutations in the context of synthetic AP3::GUS fail to exhibit detectable GUS activity at any floral stage (Fig. 5A,B). In summary, these results show that a functional CArG1, in the context of the −83 to −225 synthetic *AP3* promoter, is necessary for detectable GUS activity.

CArG2 mutants

As with CArG1 mutations, CArG2 mutations in the context of the synthetic *AP3* promoter have a dramatic effect on the GUS pattern but in the context of the intact promoter exhibit no detectable effect. CArG2 mutations in the context of the synthetic AP3::GUS trimer do not alter the temporal pattern of GUS activity but they do alter the spatial pattern. As in wild type, GUS activity in CArG2 mutants is initially detectable during stages 3-4 (Fig. 5C). Based on the number and location of cells that exhibit GUS activity, it appears that GUS activity is detected at early stages in stamen primordia, but not in petal primordia. GUS activity is detectable at a high level in stamens through stage 7. During stages 8-9, GUS activity is confined to the connective of the anther (Fig. 5D) and GUS activity continues to be detectable in the connective until post anthesis.

CArG2 mutations in the context of the −496 AP3::GUS intact promoter have no detectable effect on the GUS pattern. In these lines, GUS activity is detectable exclusively in petals and stamens beginning at stage 3.

CArG3 mutants

Although CArG3 mutations do not alter the spatial and temporal GUS activity pattern, they do have an effect on the level of GUS activity during early floral stages. CArG3 mutations, in the context of the synthetic promoter trimer, direct GUS activity at a high level in the petals and stamens beginning at stage 3-4 (Fig. 5E). During stages 6-8, GUS activity is detected at a higher level in stamens compared to petals (Fig. 5F). Beginning in stage 8, the intensity of staining in the stamens decreases compared to that observed at earlier stages and the level of GUS activity in the petals decreases to background levels. By stage 9, GUS activity is no longer detectable in the stamens. During stage 11, however, GUS activity is again detectable in the connective of the anther and

this staining is detectable until the stamens senesce (stage 14).

The effect of mutations in CArG3 is similar in the context of the intact −496 promoter. We detect GUS activity at stage 4 at a high level in the petals and stamens. The level of GUS activity in CArG3 mutants in the −496 promoter appears to be higher than the level in the wild type −496 promoter, but lower than the level in the synthetic CArG3 mutants. Beginning at stage 8 in the intact CArG3 mutant flowers the level of GUS activity is lower compared to that observed at earlier stages and by stage 10, GUS activity in the petals and stamens is reduced to background levels.

CArG1-CArG3 double mutants

We have examined CArG1-CArG3 double mutants in the context of both the intact −496 promoter and the synthetic AP3::GUS trimer. In the context of the synthetic AP3::GUS trimer, GUS activity is not detected prior to stage 12 in CArG1-CArG3 double mutants, similar to what is observed in CArG1 mutants alone in the context of the synthetic promoter (data not shown).

Although CArG1 single mutants in the context of the −496 intact promoter have no effect on the GUS pattern, in combination with CArG3 there is a reduction in late staining. CArG1-CArG3 double mutants in the context of −496 AP3::GUS exhibit GUS activity during early stages of flower development (stages 3-6) in a pattern identical to that observed in wild type (Fig. 5G). By stage 7, however, a low level of GUS activity is detected in petals and GUS activity is undetectable in stamens (Fig. 5H). By stage 9, GUS activity is undetectable in petals. In summary, CArG1 in combination with CArG3 is necessary for a high level of GUS activity during mid and late stages of flower development.

Early expression of GUS from the synthetic *AP3* promoter is independent on *AP3* and *PI*

When −496 AP3::GUS is crossed to *ap3-3* or *pi-1*, a high level of GUS activity is detected from stages 3-6 in the primordia of petals and stamens, but at later stages GUS activity is not detected throughout most of the second and third whorl cells. GUS activity is detected, however, in cells in the receptacle at the base of the first and second whorl organs (Fig. 6A). Occasionally, GUS activity is detected in more apical positions in second whorl organs in both *ap3-3* and *pi-1* mutants at late floral stages. The GUS activity pattern is similar to the *AP3* RNA expression pattern in *ap3-3* and *pi-1* mutants (Jack et al., 1992, 1994; Samach et al., 1997). Although transcription of *AP3* during late floral stages in most second and third whorl cells is dependent on both *AP3* and *PI,* continued transcription at the base of the first whorl (or first and second whorls in *ap3-3* and *pi-1* mutants) is independent of *AP3* and *PI*.

To test whether synthetic AP3::GUS is recreating *AP3* establishment, *AP3* autoregulation, and first whorl expression, we crossed wild-type synthetic AP3::GUS to *ap3-3* and *pi-1* mutants. Kanamycin resistant F_2 *ap3-3* or *pi-1* plants exhibit GUS activity during stages 3-7 in the second and third whorl primordia. At later stages, GUS activity is not detected, even at the base of the first and second whorl organs (Fig. 6B). In summary, synthetic AP3::GUS recreates both the establishment and maintenance circuits of *AP3* in whorls two and three, but does not recreate first whorl expression.

DISCUSSION

Synthetic *AP3* promoter

In yeast, mammals and plants, MADS domain-containing transcription factors have been demonstrated to bind with high affinity to a ten base pair consensus sequence called the CArG box. Between −83 and −225 in the *AP3* promoter there are three sequences with a 9 out of 10 match to the CArG box consensus sequence. A single copy of this CArG box-containing promoter sequence, when placed upstream of a minimal promoter, is not sufficient to direct GUS activity in the flower. When the −83 to −225 promoter fragment is trimerized in tandem upstream of a minimal promoter, however, the resulting GUS activity pattern recreates the key aspects of the *AP3* expression pattern. In particular, synthetic AP3::GUS constructs direct GUS activity to petals and stamens throughout most of flower development (i.e. at both early and late floral stages).

Similar synthetic promoters have been constructed to study the regulation of developmental control genes in *Drosophila*. The 300 base pair neuroectoderm enhancer (NEE) of the *Drosophila* gene *rhomboid* contains four binding sites for the Dorsal activator protein and five binding sites for bHLH activator proteins such as Twist (Ip et al., 1992). A single copy of a 57 base pair synthetic element (i.e. the minimal stripe unit) that contains two dorsal binding sites and two bHLH binding sites, when placed upstream of a minimal promoter, directs weak neuroectodermal expression. When this 57 base pair fragment is dimerized or trimerized in tandem, however, it directs reporter expression in a spatial and temporal pattern that is indistinguishable from the full length NEE (Szymanski and Levine, 1995).

The fact that multiple copies of these promoter elements are required to generate the proper spatial and temporal pattern has implications for how the activator proteins that bind to these promoter elements function to stimulate transcription. From our experiments, it is not clear whether the synergistic interaction is due solely to the increased number of binding sites or whether linkage of these binding sites is important. This can be tested by increasing the distance between the CArG box-containing monomers. In either case, transcription could be stimulated simply by providing additional binding sites for the activators which would enhance interactions with components of the transcription machinery. The binding of these activators may or may not be cooperative, but if they are cooperative between elements, it would provide an explanation for the synergistic interactions. It is also possible that the synergistic effects occur among the elements themselves rather than among individual binding sites; for example, tandem arrays of promoter elements might be more efficient at recruiting adaptors or components of the basal transcription machinery.

CArG box mutations

Evidence that the three CArG boxes in the *AP3* promoter are functionally important comes from analysis of constructs that contain CArG box mutations. The effect of the CArG mutations is very dramatic in the context of synthetic AP3::GUS construct but in the context of intact AP3::GUS the CArG mutations have either subtle effects or no detectable effect suggesting that there are redundant elements in the intact

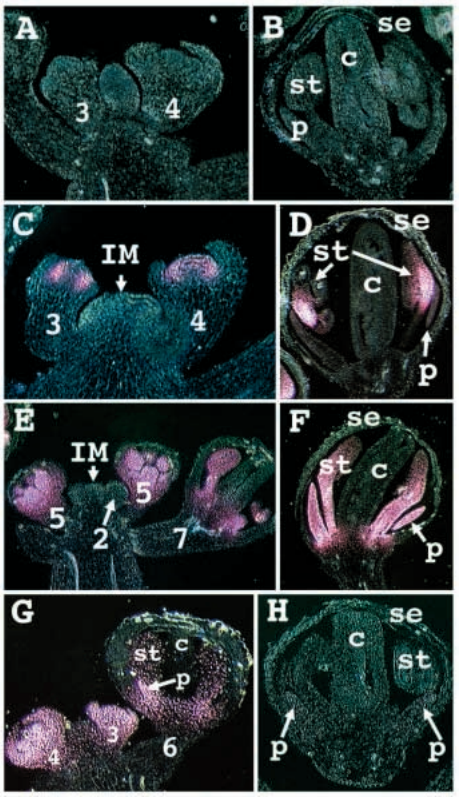

Fig. 5. AP3::GUS plants containing CArG box mutations. (A) Inflorescence from a plant that contains a CArG1 mutation in the context of the −83 to −225 synthetic *AP3* promoter. GUS activity is not detected at any stage in these mutants. (B) Single stage 8 flower from a plant that contains a CArG1 mutation in the context of the −83 to −225 synthetic *AP3* promoter. GUS activity is not detected. (C) Inflorescence from a plant that contains a CArG2 mutation in the context of the −83 to −225 synthetic *AP3* promoter. GUS activity in these flowers is detected in the stamens but not in the petals during early and mid stages of flower development. In both stage 3 and stage 4 flowers GUS activity is detected in the precursor cells for the stamens. (D) Single stage 9 flower from a plant that contains a CArG2 mutation in the context of the −83 to −225 synthetic *AP3* promoter. At this stage, GUS activity is detected in the connective of the stamen. No GUS activity is detected in petals. (E) Inflorescence from a plant with a CArG3 mutation in the context of the −83 to −225 synthetic *AP3* promoter. In CArG3 mutant flowers there is an increase in the level of GUS activity in the petals and stamens during early floral stages. (F) Single stage 8 flower from a plant with a CArG3 mutation in the context of the −83 to −225 synthetic *AP3* promoter. GUS activity is detected at a high level in the petals and stamens of mid to late stage flowers. (G) Inflorescence from a plant with a double CArG1-CArG3 mutation in the context of the −496 *AP3* promoter. GUS activity is detected during early stages (stages 3-5) in the petal and stamen primordia. In the stage 6 flower, the level of GUS activity is lower, particularly in stamens. (H) Single stage 8 flower from a plant with a double CArG1-CArG3 mutation in the context of the −496 *AP3* promoter. A very low level of GUS activity is detected in petals but GUS activity is not detected in stamens of mid to late stage flowers.

promoter that can substitute for the non-functional CArG boxes.

In molecular terms, the regulatory function of CArG3 is

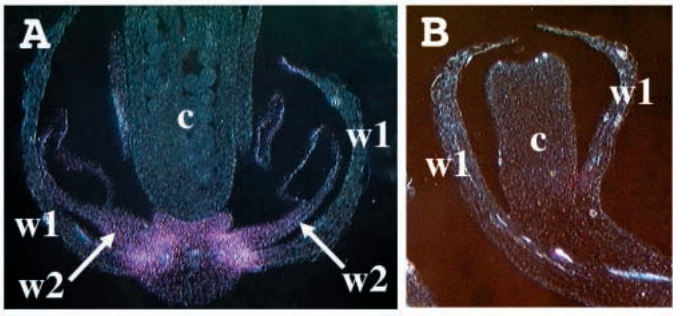

Fig. 6. Late expression in *ap3-3* and *pi-1* mutants. (A) −496 AP3::GUS *ap3-3* flower at stage 12. GUS activity is detected at high levels in the receptacle at the base of the first and second whorl organs. (B) Synthetic AP3::GUS *pi-1* flower at stage 8. A very low level of GUS activity is detected at the base in the second whorl organs. At later stages, GUS activity is not detected.

most easily explained by postulating that CArG3 is the binding site for a repressor that is required to maintain a proper level of *AP3* expression during early floral stages (Fig. 7). If mutations are present in CArG3, this repressor is unable to bind and as a result, GUS is transcribed at a higher level during early floral stages. The potential biological importance of this finding is unclear; there is no evidence that either increasing (e.g. 35S::AP3) or decreasing (e.g. *ap3-3*/+) the levels of *AP3* in whorls two and three has an effect on the development of petals and stamens.

In molecular terms, the CArG1 and CArG2 results are most easily explained by postulating that CArG1 and CArG2 are the binding site for an activator or activators that are important both for establishment and maintenance of *AP3* expression (Fig. 7). During the establishment phase, CArG1 could be the binding site for a MADS domain activator. During the maintenance phase, the simplest molecular model is that CArG1 is the binding site for the AP3/PI heterodimer. Similarly, during the establishment phase CArG2 could be the binding site for a MADS domain containing activator necessary for activation of *AP3* in petals. During the maintenance phase, the role of CArG2 is less clear. CArG2 mutations do not completely disable autoregulation since GUS activity is detected in stamens during both early and late stages suggesting that autoregulation in the third whorl is normal. Instead, it is more likely that the CArG2 mutation disrupts a petal-specific element that is required for expression during both early and late stages.

Redundancy of CArG box function is suggested by the reduced late staining in CArG1-CArG3 double mutants in the context of −496 AP3::GUS. By contrast, CArG1 and CArG3 single mutants in the −496 AP3::GUS context exhibit wild-type staining during mid to late stages of flower development. The differences in the late staining patterns suggest that disruption of either CArG1 or CArG3 can be compensated for by a functional copy of the other.

Is CArG2 a binding site for MADS domain factors?

CArG2 mutations in the context of the synthetic promoter result in a decrease in GUS activity in petals at all floral stages. The fact that CArG2 is the only CArG box that is completely

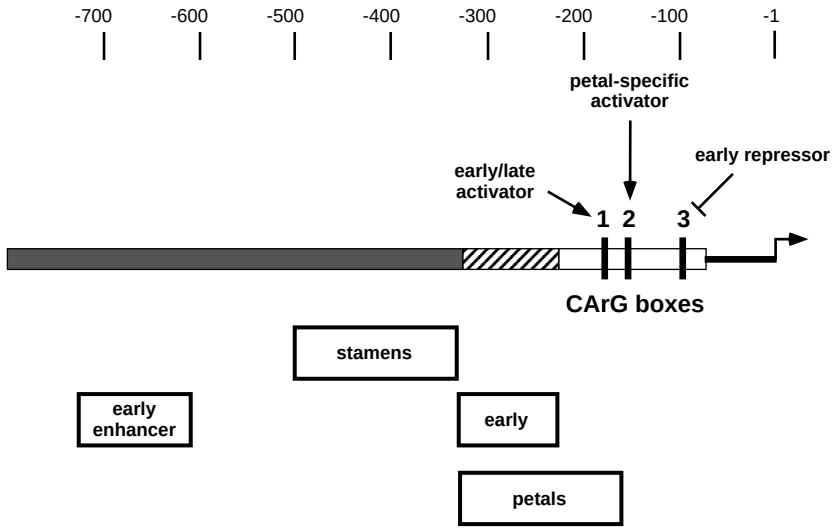

Fig. 7. Major controlling sequences in the *AP3* promoter. This schematic diagram summarizes important promoter elements in the *AP3* promoter. Boxes indicate promoter elements necessary for expression in stamens, petals and during early stages of flower development. Analysis of mutations in the three CArG boxes in the *AP3* promoter suggests that CArG1 is a binding site for a MADS domain activator during both early and late floral stages, CArG2 a binding site for a petal-specific activator, and CArG3 a binding site for a repressor that controls the level of expression during early floral stages.

conserved between *Arabidopsis AP3* and *Brassica BobAP3* suggest that it might be functionally important (Hill et al., 1998). We did not, however, detect binding of the AP3/PI proteins to wild-type CArG2 sequences in vitro. There are several possible explanations for this result. First, perhaps MADS domain proteins other than AP3/PI bind to CArG2 in vivo to mediate these effects. It has been demonstrated that different MADS domain proteins bind with different affinity to different CArG box sequences (Riechmann et al., 1996b), but in general, the sequences recognized by different MADS proteins are largely overlapping. Although it is formally possible that MADS domain proteins other than AP3 and PI bind to CArG2, this explanation seems unlikely based on present evidence. Second, perhaps coactivators are present in vivo which increase the affinity of binding of AP3/PI (or other MADS domain protein) to CArG2; the failure to detect binding of AP3/PI to CArG2 in an EMSA assay could be due the absence of such a co-activator. A third possibility is that the CArG2 mutation disrupts the binding of a non-MADS transcription factor. In designing the CArG box mutations we assumed that we would specifically be disrupting the binding of a MADS transcription factor. These mutations, however, could also be disrupting the binding of other necessary transcription factors. For all three CArG box mutations we are unable to rule out the possibility that the effects we are observing are due to the failure of non-MADS transcription factors to bind to these sequences.

Organ specific elements in the *AP3* promoter

Several lines of evidence support the hypothesis that there is a promoter element between −332 and −496 that directs expression to stamens during late stages of development (Fig. 7). First, 5′ promoter deletions to −496 direct a high level of GUS activity in petals and stamens but deletions to −332 result in GUS activity at a high level in petals, but stamen staining is reduced to a very low level. Second, fusion of promoter fragments that contain the −332 to −496 promoter piece 5′ to a minimal promoter directs GUS activity to stamens during late floral stages. Third, when the −332 to −496 promoter piece is trimerized and placed upstream of a minimal promoter, a high level of GUS activity is observed in late anthers.

5′ deletion analyses also suggest the presence of an element between −225 and −332 that is necessary both for the enhancement of the signal in the petals and for expression during early stages of development (prior to stage 5). As a test of sufficiency, the −225 to −332 promoter fragment was placed 5′ to a minimal promoter. A single copy of the −225 to −332 fragment fused to a minimal promoter fails to direct GUS activity in the flower. A tandem trimer of the −225 to −332 fragment fused to a minimal promoter directs GUS activity primarily to petals beginning at stage 6. Based on this, we conclude that the −225 to −332 promoter fragment is sufficient, when placed 5′ to a minimal promoter, to direct a low level of expression to petals, but is not sufficient to direct expression during early stages. Since 5′ deletions to −153 of the *AP3* promoter fail to exhibit GUS staining, additional sequences between −210 and −153 are necessary for the weak expression observed in petals and stamens in the −210 construct.

First whorl expression

In wild-type flowers, *AP3* RNA is expressed throughout much of flower development in a small number of cells at the base of the first whorl sepals (Weigel and Meyerowitz, 1993). *PI* RNA, by contrast, is not expressed in these first whorl cells in wild-type flowers (Goto and Meyerowitz, 1994). Since *PI* is not expressed in these cells, transcription of *AP3* during late floral stages must take place by a mechanism independent of *AP3/PI* autoregulation. Analysis of the GUS activity patterns in *ap3-3* or *pi-1* mutants that contain −496 AP3::GUS reveals detectable GUS activity at the base of the first and second whorl organs and occasionally in more apical positions in second whorl organs. We postulate that this late expression in *ap3-3* and *pi-1* mutants is regulated similarly to that in the *AP3* expressing cells at the base of the first whorl sepals in wild-type flowers; in other words *AP3* transcription during late floral stages is independent of AP3/PI autoregulation. In the case of *AP3*, the functional importance of this first whorl transcription during late floral stages is not clear since the AP3 protein is not detected in *ap3-3* or *pi-1* mutants later than stage 6 (Jack et al., 1994).

Synthetic AP3::GUS constructs lack first whorl expression suggesting that an element outside of the −83 to −225 region

is responsible for this expression. The lack of first whorl expression is most obvious when synthetic AP3::GUS is crossed to *ap3-3* or *pi-1*; in this case GUS activity is not detected later than stage 7 which is in sharp contrast to the GUS pattern in –496 AP3::GUS *ap3-3* or –496 AP3::GUS *pi-1* in which GUS activity persists until late floral stages.

Synthetic AP3::GUS recreates both establishment and maintenance phases of *AP3* expression

The most compelling evidence that synthetic AP3::GUS trimer recreates both the establishment and maintenance phases of the *AP3* expression pattern comes from analysis of the synthetic AP3:GUS in an *ap3-3* or *pi-1* mutant background. Early expression in synthetic AP3::GUS *ap3-3* (and AP3::GUS *pi-1*) is not due to autoregulation since *AP3* and *PI* are not functional. One possible explanation for this early expression is that it is due to signals that initially activate *AP3* during early stages of flower development (e.g. meristem identity genes such as *LFY*, *UFO* etc). The fact that CArG1 mutations in the context of synthetic AP3::GUS eliminate GUS activity at both early and late stages suggests that CArG box-binding MADS domain transcription factors might be involved in initially activating *AP3* during very early stages of flower development. At present, the best candidates for genes that initially activate *AP3* are members of the meristem identity class. The positive regulators of *AP3* initiation that have been identified, namely LFY and UFO, do not contain a MADS domain (Weigel et al., 1992; Ingram et al., 1995). Two meristem identity proteins, AP1 and CAL, do contain a MADS domain. It is unlikely, however, that AP1 alone plays an important activating role since in *ap1* mutants, *AP3* RNA is initially expressed normally at stage 3 (Weigel and Meyerowitz, 1993) and in 35S::AP1 flowers the development of petals and stamens is normal (Mandel and Yanfosky, 1995). There are, however, a number of other MADS box genes in *Arabidopsis* that have been isolated using MADS box homology whose function is just beginning to be determined (Ma et al., 1991; Rounsley et al., 1995; Kempin et al., 1997). Several of these MADS box genes (i.e. the AGLs) could encode potential regulators of *AP3* that function through the CArG boxes in the *AP3* promoter. RNA for several of the AGLs is expressed prior to the initial appearance of *AP3* RNA and these genes could potentially function as upstream activators or repressors of *AP3*. For example, the genes *AGL2* (Flanagan and Ma, 1994), *AGL4* (Savidge et al., 1995), or *AGL9* (based on the expression pattern of the *Antirrhinum* homologs *DEFH200* and *DEFH72* (Davies et al., 1996)) are expressed during stage 2, prior to the initial activation of *AP3* in the flower. It is not presently know whether any of the AGLs regulate the initial activation of *AP3*.

We thank Jose Luis Riechmann for the pSPUTK-AP3 and pSPUTK-PI plasmids and for comments on the manuscript and Vivian Irish for sharing results prior to publication. We also thank Jon Cassista and Lauren Campisi for generating and maintaining transgenic plants as well as for technical assistance. This work is supported by a grant from the National Science Foundation to TJ (IBN-9405884).

REFERENCES

Bechtold, N., Ellis, J. and Pelletier, G. (1993). *In planta Agrobacterium* mediated gene transfer by infiltration of adult *Arabidopsis* plants. *C. R. Acad. Sci. Paris* **316**, 1194-1199.

Benfey, P. N. and Chua, N.-H. (1990). The cauliflower mosaic virus 35S promoter: combinatorial regulation of transcription in plants. *Science* **250**, 959-966.

Bowman, J. L., Smyth, D. R. and Meyerowitz, E. M. (1989). Genes directing flower development in *Arabidopsis*. *The Plant Cell* **1**, 37-52.

Davies, B., Egea-Cortines, M., de Andrade Silva, E., Saedler, H. and Sommer, H. (1996). Multiple interactions amongst floral homeotic MADS box proteins. *EMBO J.* **16**, 4330-4343.

Deng, W. P. and Nickoloff, J. A. (1992). Site-directed mutagenesis of virtually any plasmid by eliminating a unique site. *Anal. Biochem.* **200**, 81-96.

Dolan, J. W. and Fields, S. (1991). Cell-type-specific transcription in yeast. *Biochim. Biophys. Acta* **1088**, 155-169.

Flanagan, C. A. and Ma, H. (1994). Spatially and temporally regulated expression of the MADS-box gene *AGL2* in wild-type and mutant *Arabidopsis* flowers. *Plant Mol. Biol.* **26**, 581-595.

Goto, K. and Meyerowitz, E. M. (1994). Function and regulation of the *Arabidopsis* floral homeotic gene *PISTILLATA*. *Genes Dev.* **8**, 1548-1560.

Gustafson-Brown, C., Savidge, B. and Yanofsky, M. F. (1994). Regulation of the *Arabidopsis* floral homeotic gene *APETALA1*. *Cell* **76**, 131-143.

Hill, T. A., Day, C. D., Zondlo, S. C., Thackeray, A. and Irish, V. F. (1998). Discrete spatial and temporal cis-acting elements regulate transcription of the *Arabidopsis* floral homeotic gene *APETALA3*. *Development* **125**, 1711-1721.

Huang, H., Mizukami, Y. and Ma, H. (1993). Isolation and characterization of the binding sequence for the product of the *Arabidopsis* floral homeotic gene *AGAMOUS*. *Nucl. Acids Res.* **21**, 4769-4776.

Huang, H., Tudor, M., Weiss, C. A., Hu, Y. and Ma, H. (1995). The *Arabidopsis* MADS-box gene *AGL3* is widely expressed and encodes a sequence-specific DNA-binding protein. *Plant Mol. Biol.* **28**, 549-567.

Huang, H., Tudor, M., Su, T., Zhang, Y., Hu, Y. and Ma, H. (1996). DNA binding properties of two *Arabidopsis* MADS domain proteins: binding consensus and dimer formation. *Plant Cell* **8**, 81-94.

Ingram, G. C., Goodrich, J., Wilkinson, M. D., Simon, R., Haughn, G. W. and Coen, E. S. (1995). Parallels between *UNUSUAL FLORAL ORGANS* and *FIMBRIATA*, genes controlling flower development in *Arabidopsis* and *Antirrhinum*. *Plant Cell* **7**, 1501-1510.

Ip, Y. T., Park, R. E., Kosman, D., Bier, E. and Levine, M. (1992). The *dorsal* gradient morphogen regulates stripes of *rhomboid* expression in the presumptive neuroectoderm of the *Drosophila* embryo. *Genes Dev.* **6**, 1728-1739.

Irish, V. and Yamamoto, Y. T. (1995). Conservation of floral homeotic gene function between *Arabidopsis* and *Antirrhinum*. *Plant Cell* **7**, 1635-1644.

Jack, T., Brockman, L. L. and Meyerowitz, E. M. (1992). The homeotic gene *APETALA3* of *Arabidopsis thaliana* encodes a MADS box and is expressed in petals and stamens. *Cell* **68**, 683-697.

Jack, T., Fox, G. L. and Meyerowitz, E. M. (1994). *Arabidopsis* homeotic gene *APETALA3* ectopic expression: transcriptional and post-transcriptional regulation determine floral organ identity. *Cell* **76**, 703-716.

Jefferson, R. A., Kavanagh, T. A. and Bevan, M. W. (1987). GUS fusions: β-glucuronidase as a sensitive and versatile gene fusion marker in higher plants. *EMBO J.* **6**, 3901-3907.

Kempin, S. A., Savidge, B. and Yanofsky, M. F. (1995). Molecular basis of the *cauliflower* phenotype in *Arabidopsis*. *Science* **267**, 522-525.

Kempin, S. A., Liljegren, S. J., Block, L. M., Rounsley, S. D., Lam, E. and Yanofsky, M. F. (1997). Inactivation of the *Arabidopsis AGL5* MADS-box gene by homologous recombination. *Nature* **389**, 802-803.

Krizek, B. A. and Meyerowitz, E. M. (1996). The *Arabidopsis* homeotic genes *APETALA3* and *PISTILLATA* are sufficient to provide class B organ identity function. *Development* **112**, 11-22.

Lee, I., Wolfe, D. S. and Weigel, D. (1997). *A LEAFY* co-regulator encoded by *UNUSUAL FLORAL ORGANS*. *Curr. Biol.* **7**, 95-104.

Leung, S. and Miyamoto, N. G. (1989). Point mutational analysis of the human c-fos serum response factor binding site. *Nucl. Acids Res.* **17**, 1177-1195.

Levin, J. Z. and Meyerowitz, E. M. (1995). *UFO*: an *Arabidopsis* gene involved in both floral meristem and floral organ development. *Plant Cell* **7**, 529-548.

Ma, H., Yanofsky, M. F. and Meyerowitz, E. M. (1991). *AGL1-AGL6*, an *Arabidopsis* gene family with similarity to floral homeotic and transcription factor genes. *Genes Dev.* **5**, 484-495.

Mandel, M. A., and Yanofsky, M. F. (1995). A gene triggering flower formation in Arabidopsis. *Nature* **377**, 522-524.

McBride, K. E. and Summerfelt, K. R. (1990). Improved binary vectors for *Agrobacterium*-mediated plant transformation. *Plant Mol. Biol.* **14**, 269-276.

Mizukami, Y., Huang, H., Tudor, M., Hu, Y. and Ma, H. (1996). Functional domains of the floral regulator AGAMOUS: characterization of the DNA binding domain and analysis of dominant negative mutations. *Plant Cell* **8**, 831-845.

Okamoto, H., Yano, A., Shiraishi, H., Okada, K. and Shimura, Y. (1994). Genetic complementation of a floral homeotic mutation, *apetala3*, with an *Arabidopsis thaliana* gene homologous to *DEFICIENS* of *Antirrhinum majus*. *Plant Mol. Biol.* **26**, 465-472.

Passmore, S., Maine, G. T., Elble, R., Christ, C. and Tye, B.-K. (1988). A *Saccharomyces cerevisiae* protein involved in plasmid maintenance is necessary for mating of MATa cells. *J. Mol. Biol.* **204**, 593-606.

Pellegrini, L., S., T. and Richmond, T. J. (1995). Structure of serum response factor core bound to DNA. *Nature* **376**, 490-498.

Pollock, R. and Treisman, R. (1990). A sensitive method for the determination of protein-DNA binding specificities. *Nucl. Acids Res.* **16**, 6197-6204.

Purugganan, M. D., Rounsley, S. D., Schmidt, R. J. and Yanofsky, M. F. (1995). Molecular evolution of flower development: diversification of the plant MADS-box regulatory gene family. *Genetics* **140**, 345-356.

Riechmann, J. L., Krizek, B. A. and Meyerowitz, E. M. (1996a). Dimerization specificity of *Arabidopsis* MADS domain homeotic proteins APETALA1, APETALA3, PISTILLATA, and AGAMOUS. *Proc. Natl. Acad. Sci. USA* **93**, 4793-4798.

Riechmann, J. L., Wang, M. and Meyerowitz, E. M. (1996b). DNA-binding properties of *Arabidopsis* MADS domain homeotic proteins APETALA1, APETALA3, PISTILLATA and AGAMOUS. *Nucl. Acids Res.* **24**, 3134-41.

Riechmann, J. L. and Meyerowitz, E. M. (1997). MADS domain proteins in plant development. *Biol. Chem.* **378**, 1079-1101.

Rounsley, S. D., Ditta, G. S. and Yanofsky, M. F. (1995). Diverse roles for MADS box genes in *Arabidopsis*. *Plant Cell* **7**, 1259-1269.

Samach, A., Kohalmi, S. E., Motte, P., Datla, R. and Haughn, G. W. (1997). Divergence of function and regulation of class B floral organ identity genes. *Plant Cell* **9**, 559-570.

Savidge, B., Rounsley, S. D. and Yanofsky, M. F. (1995). Temporal relationship between the transcription of two *Arabidopsis* MADS box genes and the floral organ identity genes. *Plant Cell* **7**, 721-733.

Schwarz-Sommer, Z., Huijser, P., Nacken, W., Saedler, H. and Sommer, H. (1990). Genetic control of flower development by homeotic genes in *Antirrhinum majus*. *Science* **250**, 931-936.

Schwarz-Sommer, Z., Hue, I., Huijser, P., Flor, P. J., Hansen, R., Tetens, F., Lönning, W.-E., Saedler, H. and Sommer, H. (1992). Characterization of the *Antirrhinum* floral homeotic MADS-box gene *deficiens* : Evidence for DNA binding and autoregulation of its persistent expression throughout flower development. *EMBO J.* **11**, 251-263.

Shiraishi, H., Okada, K. and Shimura, Y. (1993). Nucleotide sequences recognized by the AGAMOUS MADS domain of *Arabidopsis thaliana in vitro*. *Plant J.* **4**, 385-398.

Shore, P. and Sharrocks, A. D. (1995). The MADS-box family of transcription factors. *Eur. J. Biochem.* **229**, 1-13.

Sieburth, L. E. and Meyerowitz, E. M. (1997). Molecular dissection of the *AGAMOUS* control region shows essential *cis* elements for spatial regulation are located intragenically. *Plant Cell* **9**, 355-365.

Smyth, D. R., Bowman, J. L. and Meyerowitz, E. M. (1990). Early flower development in *Arabidopsis*. *Plant Cell* **2**, 755-767.

Szymanski, P., and Levine, M. (1995). Multiple modes of dorsal-bHLH transcriptional synergy in the *Drosophila* embryo. *EMBO J.* **14**, 2229-2238.

Theißen, G., Kim, J. T. and Saedler, H. (1996). Classification and phylogeny of the MADS-box multigene family suggest defined roles of MADS-box gene subfamilies in the morphological evolution of eukaryotes. *J. Mol. Evol.* **43**, 484-516.

Treisman, R. (1986). Identification of a protein-binding site that mediates transcriptional response to the c-*fos* gene to serum factors. *Cell* **46**, 567-574.

Treisman, R. (1992). The serum response element. *Trends Biochem. Sci.* **17**, 423-426.

Tröbner, W., Ramirez, L., Motte, P., Hue, I., Huijser, P., Lönnig, W.-E., Saedler, H., Sommer, H. and Schwarz-Sommer, Z. (1992). *GLOBOSA*: a homeotic gene which interacts with *DEFICIENS* in the control of *Antirrhinum* floral organogenesis. *EMBO J.* **11**, 4693-4704.

Valvekens, D., Van Montagu, M. and Van Lijsebettens, M. (1988). *Agrobacterium tumefaciens*-mediated transformation of *Arabidopsis thaliana* root explants by using kanamycin selection. *Proc. Natl. Acad. Sci. USA* **85**, 5536-5540.

Weigel, D., Alvarez, J., Smyth, D. R., Yanofsky, M. F. and Meyerowitz, E. M. (1992). *LEAFY* controls floral meristem identity in *Arabidopsis*. *Cell* **69**, 843-859.

Weigel, D. and Meyerowitz, E. M. (1993). *LEAFY* activates floral homeotic genes in *Arabidopsis*. *Science* **261**, 1723-1726.

Weigel, D. and Meyerowitz, E. M. (1994). The ABCs of floral homeotic genes. *Cell* **78**, 203-209.

Wynne, J. and Treisman, R. (1992). SRF and MCM1 have related but distinct DNA binding specificities. *Nucl. Acids Res.* **20**, 3297-3303.

Yanofsky, M. F., Ma, H., Bowman, J. L., Drews, G. N., Feldmann, K. A. and Meyerowitz, E. M. (1990). The protein encoded by the *Arabidopsis* homeotic gene *AGAMOUS* resembles transcription factors. *Nature* **346**, 35-39.

Yanofsky, M. F. (1995). Floral meristems to floral organs: genes controlling early events in *Arabidopsis* flower development. *Ann. Rev. Plant Physiol. Plant Mol Biol.* **46**, 167-188.

Zachgo, S., de Andrade Silva, E., Motte, P., Tröbner, W., Saedler, H. and Schwarz-Sommer, Z. (1995). Functional analysis of the *Antirrhinum* floral homeotic *DEFICIENS* gene in vivo and in vitro by using a temperature-sensitive mutant. *Development* **121**, 2861-2875.